

CONDITION ASSESSMENT APPLICATION OF STEEL SHEAR WALLS WITH SLITS

A. Jacobsen¹, T. Hitaka², M. Nakashima³, J. McCormick⁴, T. Wang⁵ and Y. Murata⁶

¹ Graduate Student, Disaster Prevention Research Institute, Kyoto University, Kyoto, Japan

² Associate Professor, Disaster Prevention Research Institute, Kyoto University, Kyoto, Japan

³ Professor, Disaster Prevention Research Institute, Kyoto University, Kyoto, Japan

⁴ Assistant Professor, Dept. of Civil and Env. Engineering, University of Michigan, Ann Arbor, USA

⁵ JSPS Post Doctoral Fellow, Disaster Prevention Research Institute, Kyoto University, Kyoto, Japan

⁶ Graduate Student, Disaster Prevention Research Institute, Kyoto University, Kyoto, Japan

Email: andres.jacobsen@kt5.ecs.kyoto-u.ac.jp

ABSTRACT :

The objective of this research is to identify the maximum drift angle sustained by a story level during an earthquake event. To accomplish this, strain patterns in suitably modified steel shear walls with slits are studied. The modifications introduced to the slit configuration were determined by means of FEM analysis. From the strain history obtained, yield zones were recorded as black and white pictures. The picture was later fed to an artificial neural network to associate each pattern to a drift angle. Analysis results were satisfactory with an accuracy of 0.25%.

Paint is suggested for the purpose of identifying the strain zones in the slit walls. The strain induces flaking in the paint, leaving patterns that can be associated with different drift angles. Qualitative characteristics such as brittleness and a consistent strain-stress relation are desirable in the paint. Coupon test results confirm the viability of the use of paint as a recording method.

KEYWORDS:

Condition assessment, steel, shear wall, pattern recognition

1. INTRODUCTION

Structural condition assessment focuses on techniques for the evaluation of the state of a structure after an earthquake event to ascertain the danger it represents for re-occupation of the building. This evaluation can be performed through health-monitoring devices that use dynamic characteristics of the structure to estimate damage to the structure, or through performance-evaluation analyses based on computer models of the structure. These approaches, although widely used, present some disadvantages. In the case of performance evaluation, the building of computer models and evaluating them under static forces or dynamic input is a complex and time-consuming process. A faster alternative is to implement health-monitoring devices in the structures. These devices, besides providing response information allow for the identification and localization of damage within buildings. Unfortunately there is an important drawback to structural health monitoring: the technology required and the cost of implementing it restricts its use to important structures, such as large spatial structures, bridges, dams and high-rise buildings. These shortcomings are the motivation to develop a simpler method of estimating the damage sustained by a structure.

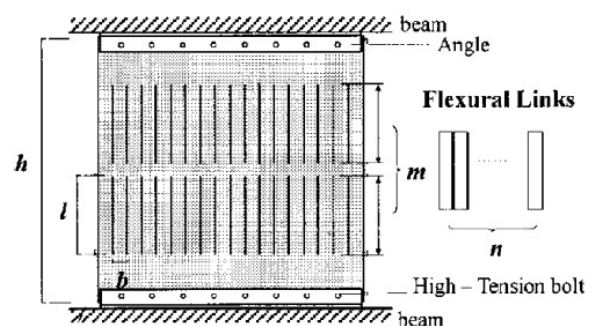
The hypothesis on which this study is based is that there is a direct relation between the strains in structural elements and their deformations. Therefore, the drift angle sustained by a story could be identified if it was possible to record the strain pattern in its shear elements. Moreover, if the strain pattern at the maximum drift level sustained by a story could be preserved, it would provide a means of inferring the damage to the structure. The realization of this idea has to overcome two challenges: first a method of extracting the

maximum strain pattern from structural elements has to be devised and second, the original hypothesis of the relation between strain patterns and drift angles has to be confirmed.

As a starting point, steel shear walls with slits (slit walls hereafter) have been considered as a potential condition assessment device (Fig. 1). The original purpose of slit walls is to be used as dampers. In this system, the steel plate segments between the slits behave as a series of flexural links, which undergo large flexural deformations relative to their shear deformation providing a ductile response without the need for significant out-of-plane stiffening of the wall. Paint is applied to the slit wall to identify high strain zones. The zones with high strains induce flaking in the paint. As the paint flaking is irreversible the maximum strain pattern is recorded and thus can be associated with the maximum drift angle. This study examines the feasibility of the proposed method, focusing on paint flaking behavior and strain patterns in slit walls.



(a) Slit wall application



(b) Slit wall schematics

Figure 1. Slit Walls

2. PAINT AS A STRAIN RECORDING METHOD

2.1. Objectives

The objective of this stage of the research is to estimate the viability of using commercially available paints as a strain-recording method, focusing on the selection of a compound that reacts to strain, an experimental testing procedure, and an analytical verification of the experimental results. The research aims for several characteristics in the paint that are fundamental for condition assessment. The objectives can be summarized as: 1) a stable strain/stress behavior in order to provide results that are comparable among similar test specimens; 2) flaking has to initiate at low levels of strain to make the strain recording compatible with strain levels developed in steel; 3) flaking has to be localized in the zones that show higher strains and do not spread to lower strain zones.

2.2. Experimental Setup

A parametric study composed of sixty pure tension tests was carried out on steel coupons. On these coupons a 100 mm strip of paint was applied in the central zone to evaluate the behavior of paint under strain. Each painted coupon represents different characteristics of thickness, composition and application technique. Two types of 2.3 mm thick steel coupons were tested: a) a standard steel coupon with a 150 mm by 60 mm steady-strain zone, and b) a coupon with the same characteristics but with a 30 mm slit in the center zone intended to study the behavior of paint under strain concentrations and verify that the strain patterns observed after the experiment represent the strain distribution predicted using finite element models.

The thickness of the layer of paint was measured at nine locations throughout the test strip. The thickness was measured seven days after the application of the paint and the tests were conducted within 10 days of the application of the paint. The average thickness for all the specimens was 70 μm . Testing was conducted in a universal testing machine. Forces and strains were measured in all the specimens. The force was measured

through a load cell installed in the loading platform. Strains were measured through strain gauges attached to the backside of the specimens. All tests were recorded using a video camera to track the behavior of paint; these recordings were later synchronized with the readings from the load cell and strain gauges. Thus, in the post-processing strain levels can be associated with qualitative characteristics of the paint such as cracking or flaking.

2.3. Experimental Procedure

Within the testing, three different phases can be identified, the first one consisting of a parametric study of the types of paint to be used and on the influence of the thickness of the layer on the behavior of paint. The thickness was controlled by the number of layers of paint applied with a spray gun (from 1 to 4). The second phase evaluates the possibility of including filler and gridlines to the compound. The final phase addresses the issue of the stability of the strain patterns obtained through paint flaking.

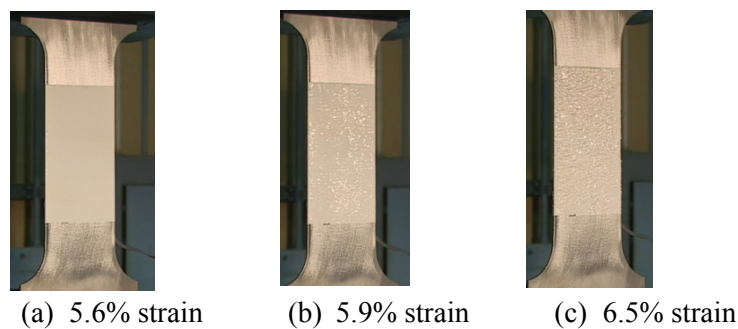


Figure 2. Response of lacquer under different levels of strain

Two parameters are considered in the first phase, the first being the paint compound (lacquer, poster color, urethane, acrylic and epoxy). The second parameter is the thickness of the paint; most of the specimens ranged between 20 and 120 micrometers. Nine of the 30 specimens tested in this stage presented visible reactions under strain; the results are summarized in Table 1. The strain levels required for visible effects in the paint were between 1.7% and 12%. Although the strain levels are higher than the original objective, these results demonstrate the viability of using paint as a method of recording strains.

Table 1. Results from first stage of tests

Paint	Avg. thickness (μm)	Flaking strain
	107.7	3.82%
Lacquer	85.2	4.98%
(30% thinner)	47.7	4.39%
	23.6	6.94%
Lacquer	51.3	1.77%
(60% thinner)	28.2	2.68%
	20.2	5.34%
Lacquer (resin)	74.9	5.21%
Poster color	118.2	12.24%

Figure 2 illustrates the behavior of a lacquer specimen. In this figure three sequential images this specimen are shown. The thickness of the paint was $20\mu\text{m}$. As opposed to some poster color specimens where effects on the paint develop slowly for strains between 12% and 30%, in these specimens the cracks develop quickly throughout the painted zone for strains between 5.6% and 6%. After the cracks develop, there are no further distinguishable effects on the paint as the strain increases. It is recognized from the results obtained in this set

of experiment that a trend exists, suggesting that as the average thickness of the film of paint increases, the minimum strain required for the paint to present visible effect decreases. It is also apparent that the most adequate paint is the combination of lacquer and thinner, as these specimens were the most successful in flaking when subjected to strain.

Table 2. Results from the third stage of tests

Paint	Avg. thickness (μm)	Flaking strain
Lacquer grid	58.2	0.14%
	68.0	0.27%
	64.6	0.14%
	60.8	0.15%
Lacquer grid (SL)	67.7	0.34%
	74.7	0.26%
	72.1	0.43%
	72.1	0.23%

In the second phase of the study filler and gridlines were added to the compound selected in the previous phase. Filler is a fine granulometry powder that is added to the compound: three different types of fillers were used (silica A and E, and talc T). Gridlines are introduced with a cardboard cutter after the paint has dried in order to introduce artificial border conditions and limit the strain distribution to a fixed strip of paint. Two-millimeter wide gridlines were used for the experiments. From the results obtained in this stage, it was concluded that the inclusion of gridlines reduces the flaking strain of paint from an average of 5.86% obtained in the previous phase to an average of 0.74%, which makes it a suitable improvement for recording strains. It is also apparent that neither the inclusion of filler nor the combination of filler and grid provide any reduction in the flaking strain. Based on the aforementioned observations it was decided not to use filler in further tests.

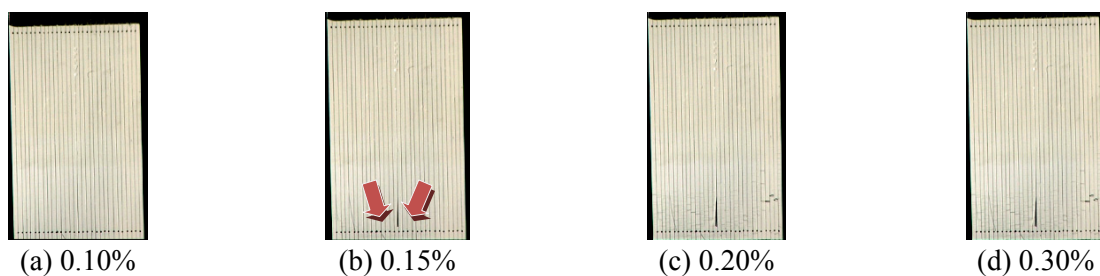


Figure 3. Paint flaking induced by strain: lacquer (50% thinner) grid (60.8 μm)

The last stage of the study consisted of eight specimens of lacquer with a 50% concentration of thinner, using 2mm vertical gridlines, which was considered the most suitable compound to record strains. Four of these specimens were standard coupons and the other four were slitted coupons. Taking into consideration the results from the previous stages, it was concluded the ideal thickness ranges between 60 μm and 100 μm . Table 2 summarizes the results for these tests. The average flaking strain was 0.31% with a standard deviation of 0.10%. These results provide confirmation of the viability of paint for recording strains. Figure 3 shows the flaking progress of one of the standard coupon tests. Figure 3a shows a picture at 0.10% strain where no flaking is apparent. Figure 3b shows the initiation of flaking in the lower left corner, where five strips begin to crack (left arrow) and one of the strips begin detaching itself from the steel plate (right arrow); at 0.20% strain (Fig. 3c) the cracking is apparent in all the lower section of the painted zone. Figure 3d shows cracking throughout the painted zone for 0.30% strain.

The slitted coupon specimens are intended to study the capacity of paint to represent strain patterns and to study the behavior of paint under strain concentrations. The responses of all slitted coupon tests show a clear indication of the strain zones (Fig. 4a). It is also noteworthy that the cracking does not propagate to zones

where strains are lower than the calculated threshold of 0.30% (Fig. 4b). A finite elements model (FEM) was constructed in ABAQUS to verify the correct determination of the strain pattern shown by the cracked paint in the coupon. The model was subjected to axial loading in the same fashion as the tested specimen. Figures 5a and 5b show a comparison between the FEM model, where in color are shown the strains above yield (0.20%), and one of the slitted specimens as seen after the detached paint had been scrapped.

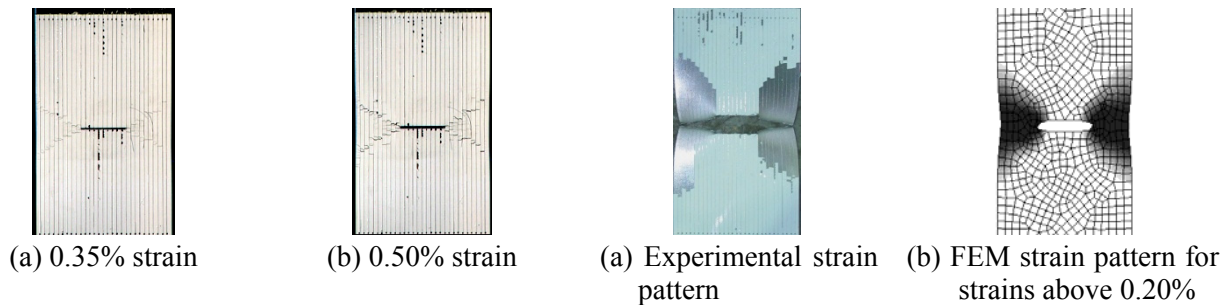


Figure 4. Paint flaking induced by strain: lacquer (50% thinner) grid - slit (74.7 μm)

Figure 5. Strain pattern comparison

3. STRAIN PATTERN ASSOCIATION WITH DRIFT ANGLES

3.1. Objectives

The objective of this part of the research is to assess the viability of estimating maximum drift angles achieved by structural elements based on the patterns defined by the strain distribution throughout the element. Therefore, the research aims to refine a slit wall with a pattern that retains the hysteretic characteristics, i.e. initial stiffness, maximum strength, and dissipation capacity, of a traditional slit wall with the added capabilities for condition assessment.

Previous studies conducted on slit walls provide design directives and experimental verifications of the hysteretic performance of slit walls. In these studies stiffnesses ranging between 20 and 150 kN/mm and maximum strengths that range between 75 and 300 kN were obtained for slit walls specimens with dimensions of 600 x 600 mm and plate thickness of 4.5 mm using SS400 steel. The hysteretic characteristics of the slit wall with modified pattern should be bound by these limits.

3.2. Slit design selection

A conventional slit wall (Fig. 6) was selected as a starting point for the search of a suitable modified slit pattern. This pattern defines a slit wall with a stiffness of 136 kN/mm and maximum strength of 252 kN when using a one third scale for the model. Details about the model are summarized in Table 3. Figure 6 shows the strain distribution of the slit wall for different drift angles. In black are shown the strains that exceed the yield strain of steel. Strain concentration is observed at the end of the slits and at the base of the plate; these concentrations are associated to the disruption of the strain field produced by the slits in the first case and to the asymmetric border conditions in the second case. It is apparent that there is scarce differentiation among the strain patterns for drift angles above 1% reducing the possibilities of associating these patterns to drift angles. It is for this reason that a variation of the slit pattern might provide a strain pattern that is more suitable to condition assessment purposes by displaying strain patterns that gradually change or grow as the drift angle increases.

In order to improve the differentiation of the strain patterns shown for different drift levels, four modified slit designs were studied using ABAQUS. In models A and B the length of the slit varies along the wall, with shorter slits concentrated in the center of the slit wall for model A, and longer ones in the center for model B. In models C and D the variation is in the width of the flexural links, with wider ones in the center for model C and thinner ones for model D. The slit designs are illustrated in the first column in Fig. 7 and their

respective hysteretic characteristics are summarized in Table 4. As it can be observed in the table there is an increase of the initial stiffness (10-20%) and maximum strength (20%) for most of the models with respect to the conventional slit pattern. The exception to this rule is the reduced maximum strength reached by model A.

Table 3. Slit wall model details

Plate size	600 x 800 mm	
Plate thickness	4.5 mm	
Slit height	200 mm	
Number of slits	8	
Slit width	2 mm	
Meshing	Quad and Triangular elements	
Material Properties	σ_y	297 N/mm ²
	σ_u	392 N/mm ²
	ϵ_y	0.2%
	ϵ_u	12.4%
Boundary conditions	Bottom	Fixed
	Top	Body constraint to the top nodes, in plane rotation and displacements allowed
	Out of plane	Restrained

Several issues have to be considered when selecting a slit design for condition assessment purposes. First is the need of retaining the hysteretic properties of the slit wall according to its structural purpose, this goal has already been achieved to an acceptable degree. It is also important to maximize the reliability of the structural element, in other words, to try to reduce strain concentrations at the end of the slits or at the edges of the plate. In the case of a large earthquake event, the zones where strains are concentrated are more prone to damage and therefore produce strength deterioration of the structural element. It is therefore undesirable to obtain strain patterns where strains are concentrated in a reduced zone at the end of the slits. The third condition that is directly related to the condition assessment capability of the structural element is to provide the highest differentiation possible between the strain patterns obtained for different drift angles. Models A and B, due to their thin flexural links, show widely distributed strain concentrations at the edge of the slits. It seems apparent that model C is more appropriate than model D as the yield zone gradually spreads in the center of the slit wall as the drift angle increases. It is also worth remarking that up to a drift angle of 2% the strain patterns can be clearly distinguished.

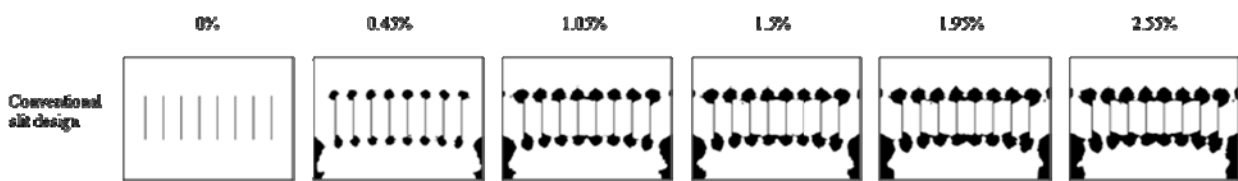


Figure 6. Strain distribution of a conventional slit design for different drift angles

3.3. Strain pattern stability

As the strain patterns evaluated in the previous section are only related to cyclic loading, it is desirable to evaluate the characteristics of the strain patterns developed under random input. In this manner, the effects of non-incremental loading can be evaluated to corroborate the assumption that strain patterns are related to the maximum drift angle experienced and are not influenced by the subsequent loading with smaller amplitudes. For this purpose, a further study was carried out considering five random inputs at three different drift levels: 0.5%, 1.0% and 1.5%. Thus, fifteen random inputs of 20 steps were generated using MATLAB, and then scaled so that the absolute maximum of each of the inputs corresponded to one of the aforementioned drift angles.

Table 4. Summary of hysteretic characteristics

		Model			
		A	B	C	D
Maximum Stiffness (kN/mm)	Initial	169	159	170	149
	Post-yielding	3.6	3.4	2.2	2.1
Maximum Strength (kN)		239.3	298.2	299.1	294.1

The results show that the strain patterns obtained for each of these drift levels resemble each other regardless of the lateral input used. Figure 8 shows the strain patterns for each drift level, gathered in a single image, where different levels of gray denote the higher likelihood for yield strains to be reached for a given drift angle. In other words, black color represents a location where yield strain was achieved for all five lateral inputs and white represents the zones where yield strain was not achieved for any lateral input. A good result is, therefore, one that shows the least amount of gray. It is also desirable to evaluate the response of the strain pattern under brief inputs. To address this issue, the slit wall was subjected to a single cycle of loading for the same previous drift levels (0.5%, 1.0% and 1.5%). The strain patterns obtained for these inputs are presented in Fig. 9. It can be observed that the strain patterns are similar to those obtained for longer inputs in the case of a drift angle of 0.5%. As the maximum drift angle increases, the strains in the middle flexural link are less apparent than for inputs with a higher number of cycles.

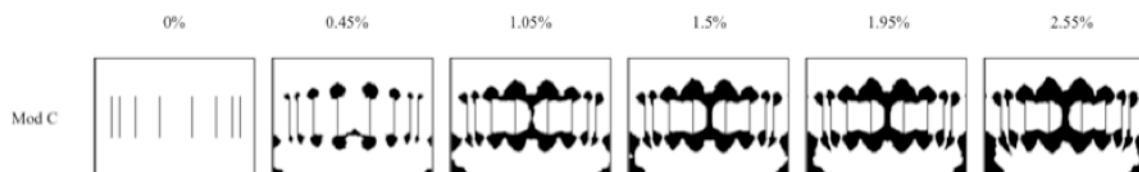


Figure 7. Strain pattern evolution for the selected slit design

3.4. Pattern recognition tools application to condition assessment

In order to provide an objective alternative to visual inspection to estimate the maximum drift angles achieved by slit walls, an artificial neural network (ANN) was trained to recognize strain patterns developed in a shear wall after it has been subjected to lateral deformation. The ANN has 3-layers and uses a back-propagating algorithm. The input vector is derived from black and white images representing the strain pattern of the slit wall. The output layer consists of a catalog of drift angles, where each drift level is associated to a pointer in the output layer. The ANN was trained with a catalog consisting of 16 drift levels between 0% and 3% (one element at every 0.2%).

For this study, 1200 images at different drift angles were generated using ABAQUS. The images capture the accumulated history of strains above the yield threshold as would be seen by the flaking of strain-sensitive paint as developed in this research. The strain patterns used belong to incremental and non-incremental cyclic loadings. One thousand of these images were used for the purpose of training. The ANN was also trained with ten sets of noisy data, i.e. images where a variable number of pixels (5-10%) were intentionally interchanged in order to emulate the unpredictability of the strain patterns as observed for the random input analysis performed in section 2.3. The two hundred remaining images were used to test the ANN with unknown subjects. Results from these test show accuracy in associating strain patterns to drift angles of

0.25%, which is slightly larger than the resolution of the drift catalog used for training. It was also found that strain patterns for drift angles above 2% are harder to identify and prone to higher errors. This shortcoming is associated with the smaller differences between strain patterns for higher drift angles.

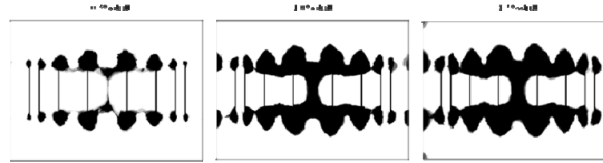


Figure 8. Cumulative stress pattern for random inputs

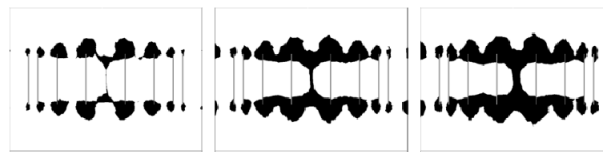


Figure 9. Stress patterns obtained for short lateral input

4. CONCLUSIONS

In this study, over sixty compounds of paint were tested under tensile strain in order to identify a strain sensitive paint for condition assessment purposes. A new slit pattern for slit walls was developed as an alternative with increased functionality as a condition assessment device.

Several conclusions can be obtained from this research: 1) Paint flaking strain is predictable within a margin of error of 0.2%. 2) A reliable paint compound, composed of lacquer with a 50% concentration of thinner and with 2 mm wide gridlines, was identified as presenting visible responses to strain. The response initiates at strains not higher than 0.4%. 3) Strain patterns identified by paint flaking resemble the strain patterns predicted by finite element models. 4) The modified slit pattern behaves similarly to the original pattern and provides a strain pattern that is more suitable for drift identification, and thus for condition assessment purposes; 5) Drift identification through neural networks provides results with an accuracy of 0.25%. 6) Higher accuracies are found for drift angles smaller than 2%.

REFERENCES

- Hitaka, T. and Matsui, C. (2003). Experimental Study on Steel Shear Wall with Slits. *Journal of Structural Engineering*, **129:5**, 586-595
- Hitaka, T., Matsui, C. and Sakai, J. (2007). Cyclic tests on steel and concrete-filled tube frames with Slit Walls. *Earthquake Engineering & Structural Dynamics*, **36:6**, 707-727
- SAC Joint Venture - Federal Emergency Management Agency (2000). Recommended Seismic Design Criteria for New Steel Moment-Frame Buildings, Report No. FEMA-350, Washington, DC, 2000
- de Joussineau, G., Petit, J.P. and Barquins, M. (2005) On the simulation of the flaking paint due to internal stresses: A simple model, *International Journal of Adhesion and Adhesives*, **25:6**, 518-526
- Kendall K. (1975) Crack propagation in lap shear joints, *Journal of Physics D*, **8:5**, 512-522
- Devos, P., Baziard, Y., Rives, B., and Michelin, P., (2001), Adherence evaluation of paint coatings using a three-point flexure test and acoustic emission, *Journal of Applied Polymer Science*, **81:8**, 1848 - 1857